

# New D– $\pi$ –A-Conjugated Organic Sensitizers Based on 4*H*-Pyran-4-ylidene Donors for Highly Efficient Dye-Sensitized Solar Cells

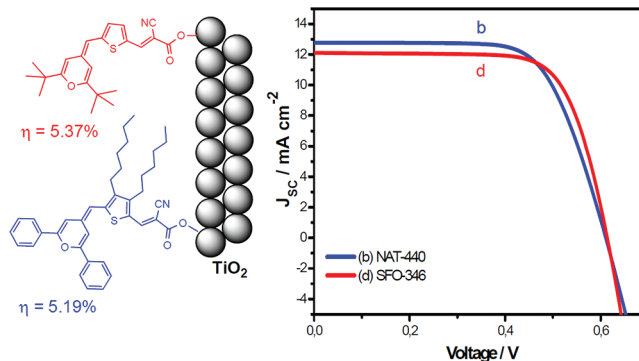
Santiago Franco,<sup>\*,†</sup> Javier Garín,<sup>†</sup> Natalia Martínez de Baroja,<sup>†</sup> Raquel Pérez-Tejada,<sup>†</sup> Jesús Orduna,<sup>†</sup> Youhai Yu,<sup>‡</sup> and Mónica Lira-Cantú<sup>\*,‡</sup>

Departamento de Química Orgánica, ICMA, Universidad de Zaragoza-CSIC, E50009 Zaragoza, Spain, Centre d'Investigació en Nanociència i Nanotecnologia (CIN2, CSIC), Laboratory of Nanostructured Materials for Photovoltaic Energy, Campus UAB E08193 Bellaterra, Barcelona, Spain

sfranco@unizar.es; monica.lira@cin2.es

Received December 9, 2011

## ABSTRACT



We have synthesized a series of four new promising D– $\pi$ –A conjugated organic sensitizers with a proaromatic 4*H*-pyran-4-ylidene as a donor, a thiophene ring in the bridge, and 2-cyanoacrylic acid as acceptor. Comparison between different donor substituents and the modification of the thiophene ring resulted in molar extinction coefficients as high as 36399 M<sup>-1</sup> cm<sup>-1</sup> at 551 nm. The photovoltaic properties of the DSSCs demonstrate power conversion efficiencies as high as 5.4%.

The conversion of solar energy to electricity appears as one of the renewable energy sources that can replace fossil fuels and directly concerns global warming. Recent progress on nanocrystalline TiO<sub>2</sub>-based dye-sensitized solar cells (DSSCs) presents an important alternative to current

solar technology because of their low-cost, lightweight, semitransparent characteristics, and potential applications.<sup>1</sup> In these cells, the sensitizer is one of the key elements for high power conversion efficiency. These devices employ mostly ruthenium complexes as charge-transfer sensitizers. Until now, only three prototype Ru complexes **N3**, **N719** and the **black dye** have achieved power conversion efficiencies over 10%. Although the ruthenium dyes exhibited high efficiency and long-term stability, they contain a limited precious metal and they are hard to purify. In this context, organic dyes are considered to be alternative photosensitizers in DSSCs owing to their ease in manufacturing and structural flexibility toward modification.

Organic dyes normally exhibit molar extinction coefficients surpassing those of ruthenium dyes and are expected

<sup>†</sup> Universidad de Zaragoza-CSIC.

<sup>‡</sup> Centre d'Investigació en Nanociència i Nanotecnologia.

(1) (a) O'Regan, B.; Graetzel, M. *Nature (London)* **1991**, *353*, 737. (b) Goetzberger, A.; Hebling, C.; Schock, H.-W. *Mater. Sci. Eng.* **2003**, *R40*, 1. (c) Robertson, N. *Angew. Chem., Int. Ed.* **2006**, *45*, 2338. (d) Imahori, H.; Umeyama, T.; Ito, S. *Acc. Chem. Res.* **2009**, *42*, 1809. (e) Yanagida, S.; Yu, Y. H.; Manseki, K. *Acc. Chem. Res.* **2009**, *42*, 1827. (f) Boschloo, G.; Hagfeldt, A. *Acc. Chem. Res.* **2009**, *42*, 1819. (g) O'Regan, B. C.; Durrant, J. R. *Acc. Chem. Res.* **2009**, *42*, 1799. (h) Mishra, A.; Fischer, M. K. R.; Bauerle, P. *Angew. Chem., Int. Ed.* **2009**, *48*, 2474. (i) Hagfeldt, A.; Boschloo, G.; Sun, L. C.; Kloo, L.; Pettersson, H. *Chem. Rev.* **2010**, *110*, 6595.

to achieve maximum power conversion efficiencies of 20.25% with absorption onset at 940 nm.<sup>2</sup> The latter make these dyes ideal molecular systems for small-molecule organic photovoltaics (OPVs).<sup>3</sup> Organic dyes with high extinction coefficients are also of high interest in solid-state dye-sensitized solar cells (ss-DSSCs) due to the requirement for thin TiO<sub>2</sub> electrodes, viscous electrolytes, or solid hole conductors.

An important factor that causes low conversion efficiency of many organic dyes in the DSSCs is the formation of aggregates on the TiO<sub>2</sub> surface. This aggregation needs to be avoided, for instance, by adding deoxycholic acid (DCA) as a coadsorbate<sup>4</sup> or by appropriate structural modifications, usually the incorporation of long alkyl chains in the spacer. It has been described that the number and position of alkyl chains linked to the thiophene improved the open circuit photovoltage ( $V_{oc}$ ) due to an effective reduction of charge recombination processes.<sup>5</sup> Recently, Tian and co-workers have reported that the aggregation between molecules can also be suppressed incorporating non planar (starburst) triaryl amines in the donor unit.<sup>6</sup>

Based on these ideas, in this communication we have designed and synthesized four new promising D- $\pi$ -A conjugated organic sensitizers (**RPT-9**, **NAT-440**, **NAT-622**, and **SFO-346**) with a 4*H*-pyran-4-ylidene as a donor, a thiophene ring in the bridge and 2-cyanoacrylic acid as acceptor. The choice of this donor moiety relies on its proaromatic character,<sup>7</sup> that is expected to improve the charge transfer process through the gain in aromaticity experienced by the donor fragment. The deliberate use of proaromatic donors for DSSCs has not yet been explored, although the photovoltaic properties of some benzothiazolylidene merocyanines<sup>8</sup> and other pyran derivatives<sup>9</sup> have been recently reported.

The aim of this work is the study of the effect of the side-chain modification of these dyes on the photovoltaic properties of dye-sensitized solar cells. Thus, we have modified the donor and the thiophene groups in these dyes. The donor group has been exchanged between a phenyl and a *tert*-butyl group, anchored to the positions 2 and 6 of the

4*H*-pyran-4-ylidene-unit, **RPT-9** and **SFO-346** dyes, respectively. The thiophene groups have been modified by the addition of two bulky hexyl groups, the **NAT-440** and **NAT-622** dyes, respectively (Figure 1). The dyes can be easily synthesized in moderate yields by well-known organic reactions including Wittig–Horner, Knoevenagel, and formylation reactions. The synthetic protocols and characterization of the dyes are provided in the Supporting Information.

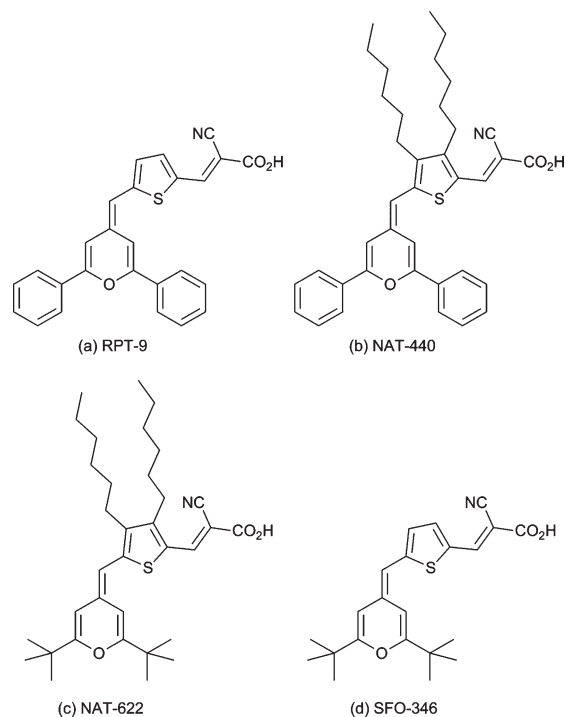


**Figure 1.** Molecular structures of the 4*H*-pyran-4-ylidene-based dyes: (a) **RPT-9**, (b) **NAT-440**, (c) **NAT-622**, and (d) **SFO-346**.

Table 1 shows the absorption and electrochemical properties of the synthesized dyes. The UV–vis spectra of the dyes in CH<sub>2</sub>Cl<sub>2</sub> (Figure 2) show an intense absorption band which can be attributed to the intramolecular charge transfer from the proaromatic donor to cyanoacrylic acid. The high molar extinction coefficient absorption bands are in favor of light-harvesting and hence photocurrent generation in DSSCs.

The redox potentials of the sensitizers were measured by differential pulse voltammetry in CH<sub>2</sub>Cl<sub>2</sub>. As shown in Table 1, the excited-state reduction potential (calculated from  $E_{ox} - E_{0-0}$ ) of the four dyes is more negative than the conduction band edge (−0.5 V vs NHE) and the ground-state oxidation potential is in all cases higher than the redox potential of the iodide/triiodide couple (+0.4 V vs NHE). These values are adequate for an effective electron injection into the semiconductor and ensure the regeneration of the oxidized form of the dyes in a DSSC.

The molecular geometries of these new organic dyes in CH<sub>2</sub>Cl<sub>2</sub> have been optimized using the B3LYP hybrid

(2) Ito, S.; Zakeeruddin, S. M.; Humphry-Baker, R.; Liska, P.; Charvet, R.; Comte, P.; Nazeeruddin, M. K.; Pechy, P.; Takata, M.; Miura, H.; Uchida, S.; Gratzel, M. *Adv. Mater.* **2006**, *18*, 1202.

(3) Buerckstuehmer, H.; Tulyakova, E. V.; Deppisch, M.; Lenze, M. R.; Kronenberg, N. M.; Gsaenger, M.; Stolte, M.; Meerholz, K.; Wuerthner, F. *Angew. Chem., Int. Ed.* **2011**, *50*, 11628.

(4) Hara, K.; Dan-oh, Y.; Kasada, C.; Ohga, Y.; Shinpo, A.; Suga, S.; Sayama, K.; Arakawa, H. *Langmuir* **2004**, *20*, 4205.

(5) (a) Wang, Z. S.; Koumura, N.; Cui, Y.; Takahashi, M.; Sekiguchi, H.; Mori, A.; Kubo, T.; Furube, A.; Hara, K. *Chem. Mater.* **2008**, *20*, 3993. (b) Choi, H.; Baik, C.; Kang, S. O.; Ko, J.; Kang, M. S.; Nazeeruddin, M. K.; Gratzel, M. *Angew. Chem., Int. Ed.* **2008**, *47*, 327.

(6) (a) Ning, Z. J.; Zhang, Q.; Wu, W. J.; Pei, H. C.; Liu, B.; Tian, H. *J. Org. Chem.* **2008**, *73*, 3791. (b) Ning, Z. J.; Tian, H. *Chem. Commun.* **2009**, 5483.

(7) Andreu, R.; Carrasquer, L.; Franco, S.; Garin, J.; Orduna, J.; Martinez, de B. N.; Alicante, R.; Villacampa, B.; Allain, M. *J. Org. Chem.* **2009**, *74*, 6647.

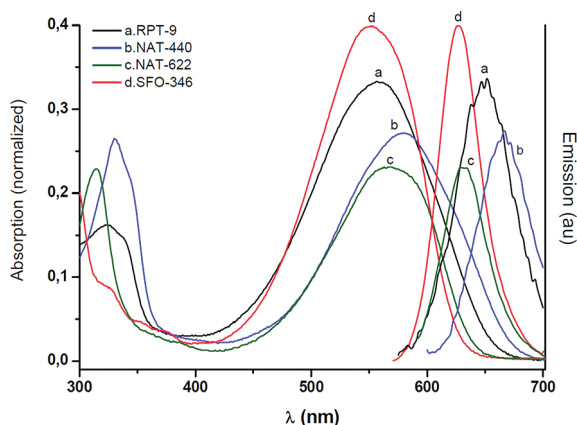
(8) Sayama, K.; Tsukagoshi, S.; Hara, K.; Ohga, Y.; Shinpo, A.; Abe, Y.; Suga, S.; Arakawa, H. *J. Phys. Chem. B* **2002**, *106*, 1363.

(9) (a) Awuah, S. G.; Polreis, J.; Prakash, J.; Qiao, Q.; You, Y. *J. Photochem. Photobiol., A* **2011**, *224*, 116. (b) Bolag, A.; Nishida, J.; Hara, K.; Yamashita, Y. *Chem. Lett.* **2011**, *40*, 510.

**Table 1.** Absorption, Fluorescence, and Electrochemical Properties of the Dyes

dye	$\lambda_{\text{abs}}^a$ (nm)	$\lambda_{\text{em}}^a$ (nm)	$\epsilon$ ( $\text{M}^{-1} \text{cm}^{-1}$ )	$E_{\text{ox}}^b$ (V) (vs NHE)	$E_{0-0}^c$ (eV)	$E_{\text{red}}^d$ (V) (vs NHE)
a <b>RPT-9</b>	556	652	33899	+0.81	2.00	-1.19
b <b>NAT-440</b>	580	667	28840	+0.83	1.94	-1.11
c <b>NAT-622</b>	584	629	23700	+0.85	2.03	-1.18
d <b>SFO-346</b>	551	627	36399	+0.86	2.05	-1.19

<sup>a</sup> Absorption and emission spectra were measured in  $\text{CH}_2\text{Cl}_2$  solutions ( $10^{-5}$  M) at room temperature. <sup>b</sup> The oxidation potentials, measured in  $\text{CH}_2\text{Cl}_2$  with 0.1 M TBAPF<sub>6</sub> as electrolyte and Ag/AgCl as reference electrode, were converted to normal electrode (NHE) by addition of 0.199 V. <sup>c</sup>  $E_{0-0}$  was estimated from the intersection between the absorption and emission spectra. <sup>d</sup> The estimated reduction potential of the dye was calculated from  $E_{\text{ox}} - E_{0-0}$ .

**Figure 2.** Absorption and emission spectra measured in  $\text{CH}_2\text{Cl}_2$  solutions ( $10^{-5}$  M) at room temperature for (a) **RPT-9**, (b) **NAT-440**, (c) **NAT-622**, and (d) **SFO-346**.

functional<sup>10</sup> and the SMD solvation model.<sup>11</sup> These calculations result in a planar conjugated  $\pi$ -system in every case. We have also calculated the lowest energy transitions using a TD-DFT approach (Table 2). Calculations predict an increase in both HOMO and LUMO energies when adding hexyl substituents or changing a phenyl by a *tert*-butyl group. Comparing to reference dye **RPT-9**, hexyl substituents on the thiophene ring (**NAT-440**) cause a bathochromic shift, while *tert*-butyl groups on the donor moiety (**SFO-346**) give rise to an hypsochromic shift, in agreement with the experimental results (see Table 1). It is also noteworthy that hexyl groups attached to the thiophene ring cause a decreased oscillator strength that correlates well with the decreased extinction coefficients of **NAT-440** and **NAT-622** as compared to **RPT-9** and **SFO-346**, respectively. The calculated molecular geometries, energies, and the molecular orbital contour plots are included in the Supporting Information.

Another important issue for a sensitizer is the photochemical and thermal stability. The thermal stabilities of the dyes were studied by thermogravimetric analysis

**Table 2.** SMD TD-B3LYP/6-31G\*\* Calculation Results in  $\text{CH}_2\text{Cl}_2$ 

dye	$\lambda_{\text{max}}$ (nm)	$f$	HOMO (eV)	LUMO (eV)	HOMO–LUMO gap (eV)
a <b>RPT-9</b>	561	1.23	-4.95	-2.56	2.39
b <b>NAT-440</b>	571	1.11	-4.85	-2.51	2.34
c <b>NAT-622</b>	534	1.02	-4.81	-2.36	2.45
d <b>SFO-346</b>	523	1.04	-4.92	-2.43	2.49

(TGA) under nitrogen, with a heating rate of 10 °C/min. The decomposition temperatures ( $T_d$ ) were estimated as the temperature that is the intercept of the leading edge of the weight loss by the baseline of the TGA scans. The results show that all the dyes described in this communication are thermally stable with decomposition temperatures higher than 135 °C ( $T_d$  (°C): **RPT-9**, 205; **NAT-440**, 189; **NAT-622**, 135; **SFO-346**, 185), in principle adequate for a photovoltaic device.

The photovoltaic performance of the sensitizers, i.e., the incident photon-to-current conversion efficiency (IPCE) and the photocurrent–voltage ( $J-V$ ) curve, was carried out in test devices using standard mesoporous 4  $\mu\text{m}$  thick  $\text{TiO}_2$  films with the iodolyte AN-50 (Solarionix) as the electrolyte. The dye adsorption on  $\text{TiO}_2$  was carried out in dichloromethane. The IPCE graphs in Figure 3 show a IPCE peak at 440 nm for the **RPT-9** and **SFO-346** with values of 53% and 62%, respectively. In the case of the sensitizers **NAT-622** and **NAT-440** the maximum IPCE peak is found at 540 nm with values very similar around 53%. In all cases, the IPCE graphs are in accordance with the shape and magnitude of the respective extinction coefficients and absorption spectra shown in Figure 2 and Table 1. The  $J-V$  curves of devices under simulated full sunlight (AM 1.5G, 100  $\text{mW}/\text{cm}^2$ ) are shown in Figure 3, and the corresponding photovoltaic parameters, i.e., the conversion efficiency ( $\eta$ ), short-circuit photocurrent density ( $J_{\text{sc}}$ ), open-circuit photovoltage ( $V_{\text{oc}}$ ), and the fill factor (ff), are given in Table 3 (average of four samples).

Taking the **RPT-9** sensitizer as the basic molecular formula for this series of compounds (Figure 1), the modification of the thiophene group of the **RPT-9** dye

(10) Becke, A. D. *J. Chem. Phys.* **1993**, *98*, 5648.

(11) Marenich, A. V.; Cramer, C. J.; Truhlar, D. G. *J. Phys. Chem. B* **2009**, *113*, 6378.

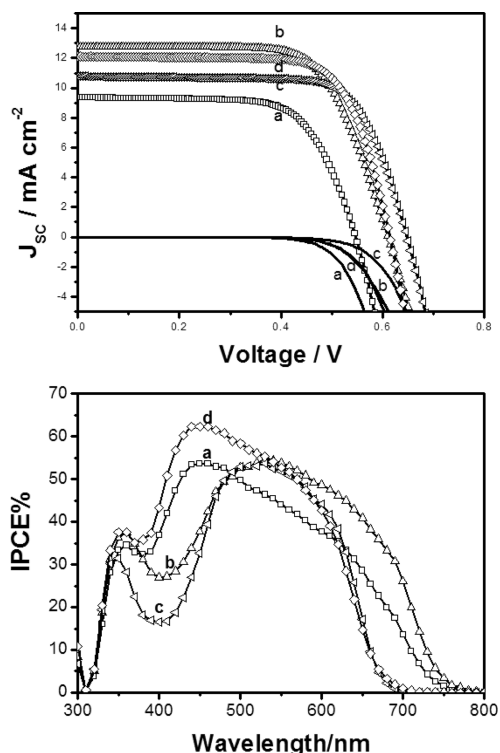


**Figure 3.** Photocurrent–voltage (above) and IPCE (below) curves of test devices with 4  $\mu\text{m}$  thick  $\text{TiO}_2$  films, sensitized with (a) **RPT-9**, (b) **NAT-440**, (c) **NAT-622**, and (d) **SFO-346** under full 100  $\text{mW cm}^{-2}$  simulated AM 1.5G sunlight.

with two bulky hexyl groups results in the **NAT-440** dye. Comparison of the absorption spectra of both sensitizers proves a red shift of the maximum from 556 nm of the **RPT-9** dye, to 580 nm for the **NAT-440**. The latter is in good agreement with the IPCE max peak shift observed from 460 to 540 nm for the same dyes, respectively. This substitution on the thiophene group allowed an impressive increase in power conversion efficiency from 3.49% to 5.19%. The replacement of the phenyl group by *tert*-butyl side group resulted in the **SFO-346** dye. In this case, an increase on the power conversion efficiency up to 5.37% obtaining a maximum in the IPCE spectra of 62% at 460 nm was observed. Nevertheless, the dual modification of the **RPT-9** dye with both, the *tert*-butyl donor group in the 4*H*-pyran-4-ylidene unit and the bulky hexyl acceptor group in the thiophene group, dye **NAT-622**, did not result in the enhancement of the power conversion efficiency. The latter is probably due to a steric effect that these modifications infuse to the final molecule.

In summary, we have successfully synthesized a series of new promising D– $\pi$ –A conjugated organic sensitizers (**RPT-9**, **NAT-440**, **NAT-622**, and **SFO-346**) with

**Table 3.** Photovoltaic Parameters of Devices with a 4  $\mu\text{m}$  Thick  $\text{TiO}_2$  Film under Simulated AM 1.5G Illumination ( $100 \text{ mW/cm}^2$ )<sup>a</sup>

dye	$V_{oc}$ (V)	$J_{sc}$ (mA)	ff	$\eta$ (%)
<b>a RPT-9</b>	$0.545 \pm 0.005$	$9.35 \pm 0.53$	$68.5 \pm 0.6$	$3.49 \pm 0.19$
<b>b NAT-440</b>	$0.595 \pm 0.007$	$12.32 \pm 0.10$	$70.8 \pm 1.1$	$5.19 \pm 0.02$
<b>c NAT-622</b>	$0.645 \pm 0.011$	$10.78 \pm 0.22$	$71.5 \pm 1.4$	$4.97 \pm 0.13$
<b>d SFO-346</b>	$0.610 \pm 0.011$	$12.10 \pm 0.29$	$72.8 \pm 1.1$	$5.37 \pm 0.11$
<b>N719</b>	$0.712 \pm 0.012$	$14.13 \pm 0.1$	$68.1 \pm 1.8$	$6.90 \pm 0.30$

<sup>a</sup>For comparison purposes the photovoltaic values of a DSSC applying the commercial **N719** dye. Average of four samples.

a 4*H*-pyran-4-ylidene as a donor, a thiophene ring in the bridge and 2-cyanoacrylic acid as acceptor. We have demonstrated photovoltaic response on these sensitizers, obtaining between  $\sim 3.5$ – $5.4\%$  conversion efficiency. We have observed that the highest photovoltaic performance is obtained when the dye shows a 2-cyanoacrylic acid substituent as the acceptor and a 4*H*-pyran-4-ylidene with two *tert*-butyl groups as the donor unit linked to the thiophene ring. The highest  $V_{oc}$  of the devices were observed for the **NAT-622** and the **SFO-346** dyes with values around 0.6 V, substantially higher than the 0.5 V observed for the basic dye molecule, **RPT-9**. The latter has been attributed to the presence of the phenyl group. Voltage values below the standard 0.75 V usually obtained for a good DSSC are an indication of charge recombination losses. The latter indicates that the application of a phenyl-based donor group results in higher recombination losses than the *tert*-butyl group.

**Acknowledgment.** We thank the Spanish Ministry of Science and Innovation, MICINN-FEDER (projects CTQ2008-02942, CTQ2011-22727 and ENE2008-04373), the Gobierno de Aragón-Fondo Social Europeo (E39), the Consolider NANOSELECT project CSD2007-00041, the Xarxa de Referència en Materials Avançats per a l'Energia, XaRMAE of the Catalonia Government for financial support. N.M.de B. thanks the Departamento Educación, Gobierno de Navarra, for a predoctoral grant. Y.Y. thanks the Spanish National Research Council (CSIC) for a JAE postdoctoral contract. R.P.T. thanks the Spanish National Research Council (CSIC) for a JAE predoctoral grant.

**Supporting Information Available.** General experimental methods, synthesis, characterization, devices, measurements, calculated molecular geometries, energies, and molecular orbital contour plots. This material is available free of charge via the Internet at <http://pubs.acs.org>

The authors declare no competing financial interest.